OPTICS

Observation of mean path length invariance in light-scattering media

Romolo Savo,[1] Romain Pierrat,[2] Ulysse Najar,[1] Rémi Carminati,[2] Stefan Rotter,[3] Sylvain Gigan[1]*

The microstructure of a medium strongly influences how light propagates through it. The amount of disorder it contains determines whether the medium is transparent or opaque. Theory predicts that exciting such a medium homogeneously and isotropically makes some of its optical properties depend only on the medium's outer geometry. Here, we report an optical experiment demonstrating that the mean path length of light is invariant with respect to the microstructure of the medium it scatters through. Using colloidal solutions with varying concentration and particle size, the invariance of the mean path length is observed over nearly two orders of magnitude in scattering strength. Our results can be extended to a wide range of systems—however ordered, correlated, or disordered—and apply to all wave-scattering problems.

The assumption that the structure of medium is inherently linked to its functional behavior lies at the heart of material engineering and has driven progress across disciplines, with numerous applications in microelectronics, photonics, medicine, atmospheric science, soft matter, solar cells, lasers, and bioimaging (*1*–*4*). This is particularly true for the properties of wave scattering through a medium, which depend very sensitively on whether a medium is homogeneous, structured, or disordered (*5*–*12*).

In stark contrast with this view, a recent theoretical study pointed out that a very fundamental property of wave transport is extremely insensitive with respect to the structure of the underlying medium (*13*). Specifically, it was shown that when all modes in a medium are equally excited, the mean path length traveled by waves inside the medium only depends on the medium's boundary geometry, not on its internal microstructure. To derive this result on a theoretical level, an invariance property first found for random walks (*14*) was generalized in (*13*) to arbitrary wave-scattering scenarios, such as for light in a disordered material (Fig. 1). In all cases, the mean length $\langle s \rangle$ of trajectories that enter the medium at arbitrary positions and incident angles up to the point where they exit the medium is predicted to be independent of whether the medium is uniform, highly structured, disordered, or anything in between. Apart from restrictions due to finite absorption, the mean path length is found to be

$$\langle s \rangle = v_E \langle t \rangle = \frac{4V}{\Sigma} \qquad (1)$$

for a three-dimensional geometry of volume V and surface Σ (*13*). Here, v_E is the transport velocity, which for wave transport in resonant media takes into account the dwell time inside the resonant particles (supplementary text S6). Brackets $\langle \ldots \rangle$ in Eq. 1 stand for averaging over all available initial positions and angles of incidence (with Lambertian distribution). For a highly structured density of states (DOS) with band gaps or pronounced resonances, additional frequency averaging is required to balance out any such system-specific features (*13*).

For optical systems, the predicted invariance property sets very rigid bounds on the optical path-length enhancement achievable by modifying the underlying medium structure. As such, this result is complementary to the conclusion reached by Yablonovitch in the context of solar cells design (also known as the Yablonovitch limit) (*15*), which predicts that the maximum energy enhancement achievable by trapping light in a medium depends only on its optical DOS, regardless of the microscopic details enabling the trapping. At the root of both results lies the equipartition theorem, which guarantees equal occupation of all optical states available in the medium, provided that the surrounding radiation field is statistically homogeneous and isotropic (a detailed derivation is provided in supplementary text S6). This particular condition, which in scattering media leads to the equipartition of optical energy on all the available light paths, can be realized in an experiment by illuminating the system so that light enters the medium from all possible directions (Lambertian illumination).

We considered the case of a fully disordered medium, in which the crossover between systems with different degrees of disorder can be described by the transport mean free path ℓ^*, which corresponds to the length after which the propagation direction of an incoming wave or particle gets randomized. Applying the theoretical predictions of Eq. 1 to this case would mean that any change of ℓ^* should leave the mean path length invariant. We investigated multiple scattering of light in colloidal suspensions of particles in water (Figs. 2 and 3). By varying the concentration and size of the particles, the mean free path is tuned by almost two orders of magnitude, covering the range from a nearly transparent to a very opaque system. We measured the mean length of light trajectories from temporal decorrelation of an optical speckle pattern in each one of these suspensions and unambiguously observed this invariance. The distribution of path lengths gets modified when changing the transport mean free path; only the mean value of the distribution stays unchanged.

When shining light on a disordered medium, the spatial inhomogeneity of the refractive index prohibits a straight-line propagation, forcing the wave instead to scatter in all available directions (Fig. 1C). To measure the resulting optical path length distribution $P(s)$, most common methods use ultrashort pulses and time-resolved detection

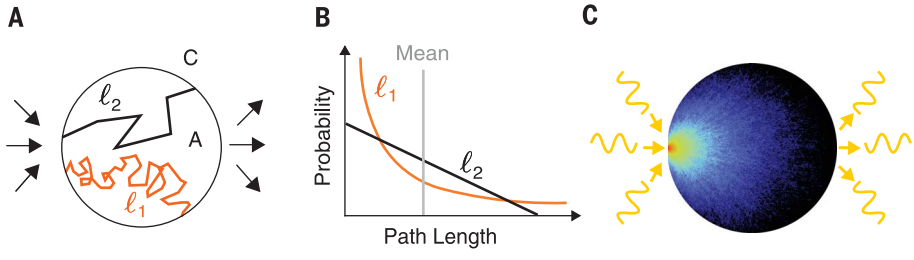

Fig. 1. Invariance of the mean path length in random walks and wave scattering. (**A**) For random walks, the mean length $\langle s \rangle$ of trajectories crossing a bounded region does not depend on the characteristic mean free path ℓ, but only on the ratio between the surface A and the perimeter C—that is, $\langle s \rangle = \pi A/C$ (in two dimensions). Two trajectories are presented corresponding to two different mean free path $\ell_2 \gg \ell_1$. For this fundamental result to hold, the mean value $\langle \ldots \rangle$ needs to include all surface positions for entering the medium and an isotropic distribution of incidence angles. (**B**) Illustration of the variation in the path length distribution for the two mean free paths ℓ_1 and ℓ_2. When changing the mean free path, the path-length distribution changes, but its mean value remains the same. (**C**) The same physics also applies to light scattering through a disordered region when the conditions for optical energy equipartition are fulfilled, here illustrated for light rays entering a circular region at a specific point with isotropic illumination.

[1]Laboratoire Kastler Brossel, École Normale Supérieure–Paris Sciences et Lettres (PSL) Research University, CNRS, Université Pierre et Marie Curie–Sorbonne Universités, Collège de France, 24 rue Lhomond, 75005 Paris, France. [2]École Supérieure de Physique et de Chimie Industrielles de la Ville de Paris, PSL Research University, CNRS, Institut Langevin, 1 rue Jussieu, 75005 Paris, France. [3]Institute for Theoretical Physics, Vienna University of Technology (TU Wien), A-1040 Vienna, Austria.
*Corresponding author. Email: sylvain.gigan@lkb.ens.fr

(*16*) or broadband sources and interferometric detection (*17*, *18*). However, we do not require access to the full distribution $P(s)$, only to its mean value $\langle s \rangle = \int_0^\infty P(s) s ds$. We therefore developed a technique derived from DWS (diffusing wave spectroscopy) (*19*, *20*) to directly measure the mean optical path length in dynamic scattering media with high sensitivity and dynamic range. In this approach, we illuminated the sample with a monochromatic laser and measured the autocorrelation function $g_E(\tau) = |\langle E^*(\tau)E(0)\rangle|^2 / |\langle EE^*\rangle|^2$ of the temporal fluctuations in the scattered light field $E(t)$. We used the connection between speckle fluctuations and the distribution of optical path lengths $P(s)$, which is formalized as

$$g_E(\tau) = \int_0^\infty ds P(s) \exp\left(-\frac{s}{\ell^*}\frac{2\tau}{\tau_0}\right) \qquad (2)$$

where $\tau_0 = 1/(k^2 D)$, k is the wave vector inside the medium, and D is the diffusion constant of the scattering particles (supplementary text S2). Quantitative information on the mean value can be immediately retrieved by considering the very early-time decorrelation. Indeed, the derivation of Eq. 2 evaluated at $\tau = 0$ leads to an explicit expression for the mean optical path length

$$\langle s \rangle = -\frac{dg_E}{d\tau}\bigg|_{\tau=0} \frac{\ell^* \lambda_0^2}{8\pi^2 n^2 D} \qquad (3)$$

where λ_0 is the light wavelength in vacuum and n is the medium refractive index. Equations 2 and 3 rely only on the so-called continuum approximation of the multiple scattering process (*21*), which in practice requires a few scattering events to be valid (*21*, *22*). Because paths with very few scattering events can contribute to the mean path length, the accuracy of Eqs. 2 and 3 has been additionally verified for all experimental situations by using Monte Carlo simulations (supplementary text S7).

The scattering solution is contained in a cylinder glass cell, which supports the liquid and defines its geometrical features (Fig. 2A). In this elongated geometry, the V/Σ ratio simplifies into $R/2$, where R is the cylinder radius and the expected mean path length from Eq. 1 is $s = 2R$. Because of the index mismatch between the scattering medium, the glass cell, and the outer regions, Eq. 1 cannot be directly applied because of multiple boundary reflections. We therefore developed a more refined model that takes into account correct boundary conditions, which shows that the invariance property remains valid in the presence of interfaces. For the simple case of a single boundary, it leads to $\langle s_{\mathrm{theo}} \rangle = v_E \langle t \rangle = (4V/\Sigma)(n_2^2/n_1^2)$, where n_1 and n_2 are the refractive index of the outer and of the scattering regions, respectively (supplementary text S6). Here, we are in the more complex situation of multiple boundaries (medium-glass-air); furthermore, our technique only gives access to the light path inside the scattering region (not in the glass part). Nonetheless, Monte Carlo simulations allowed us to find the expected invariant mean path length $\langle s_{\mathrm{in}} \rangle$. Qualitatively, the presence of boundaries means that light exiting the scattering region has a probability to be reflected back to propagate again into the scattering medium; therefore, $\langle s_{\mathrm{in}} \rangle$ is larger compared with the ideal case, in which all trajectories hitting the boundaries leave the region (*13*, *14*).

The sample is illuminated with a laser light sheet all along its diameter so that light enters with all possible angles with respect to the surface normal. To collect light from all surface locations, we used a multimode fiber (10 micrometers core) mounted sufficiently far away from the sample and placed on a goniometric mechanical arm for angle-resolved measurements. The multimode fiber guides light to single-photon counters, and a coincidence electronics allows us to measure the temporal autocorrelation (supplementary text S1 and S3).

An example of measurements for a sample with $\ell^* \approx 500$ micrometers for detection angles ranging from 0° (forward direction) to 175° (backward direction) is shown in Fig. 2B. For this rather opaque sample, $2R/\ell^* \approx 20$, the characteristic decorrelation time of the autocorrelation function ranges from tens of microseconds in the forward direction to some milliseconds in the backward direction. The decorrelation time decreases when the number of scattering events increases, so our results provide evidence of the variation in the average number of scattering events between transmitted and reflected light. We adopted Eq. 3 to measure the mean optical path length at each angle and evaluated the derivative of the autocorrelation at the origin as the slope of a linear

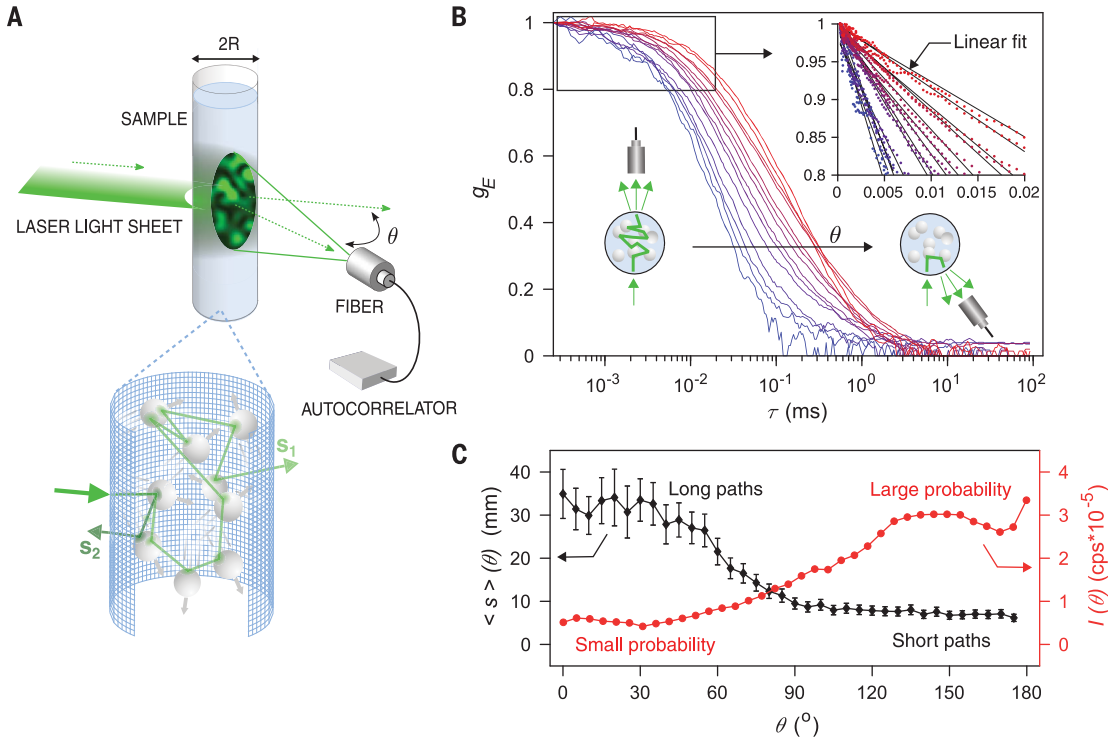

Fig. 2. Measurement of the mean optical path length in dynamic disordered media. (**A**) Samples consist of water-dispersed polystyrene microbeads contained in a cylindrical glass cell of internal diameter $2R = 8.54$ mm. Trajectories are represented as long trajectories leaving the sample in transmission (s_1) and short trajectories leaving the sample in reflection (s_2). The fiber rotates around the sample to collect light (from 0° to 175°), which is guided to an autocorrelator. (**B**) Field autocorrelation at increasing angles (x axis in log-scale). For clarity, only some selected curves are shown. (Inset) The mean optical path length is extracted from the slope of a linear fit at very early times. (**C**) Angle-dependent mean optical path length (black diamonds) and corresponding scattered light intensity (red circles) measured at steps of 5°. Error bars give 95% statistical confidence and are calculated by propagating the experimental errors that contribute—the error on the linear fit performed in (B) and errors on the measurements of ℓ^* and D. Errors on intensities are of a few percent and appear smaller than the markers.

fit of the first measured points, as shown in the closeup of Fig. 2B (supplementary text S4). The multiplicative coefficient in Eq. 3 containing ℓ^* and D was measured with an independent characterization of the sample (supplementary text S5). The recorded angular mean path lengths—together with the corresponding scattered light intensity, which quantifies the probability to have light exiting in this particular direction (Fig. 2C)—show that long trajectories, which contribute to the overall mean with large values, are less probable than short trajectories, which in turn are more abundant but contribute to the overall mean with small values. This feature illustrates the delicate balance between long and short trajectories that enables the mean value to be independent of the actual path-length distribution and that is at the root of this invariance property.

The most striking feature appears when considering the variation of both the angular mean path length and the corresponding intensity for different values of the transport mean free path ℓ^* (Fig. 3, B and C). Starting from the most opaque sample, and decreasing the scattering strength (for increasing transport mean free path), both the path length curve as well as the associated intensity get more symmetrically distributed among all angles. Then, when the transport mean free path becomes comparable with the sample size, the symmetry of the angular mean path length curve becomes completely inverted as the sample becomes more transparent, and longer path lengths are observed in reflection rather than in transmission. The symmetry of the intensity in turn is inverted in the opposite sense so as to completely compensate the redistribution of path lengths. In our analysis, we measured the overall mean path length over all trajectories; therefore, these two distributions get convolved in a weighted angular average. This average is thus evaluated by multiplying the angle-dependent values of Fig. 3B with the intensities of Fig. 3C as weighting functions: $\langle s_{\mathrm{exp}}\rangle = \sum_i \langle s\rangle(\theta_i) I(\theta_i) \Big/ \sum_i I(\theta_i)$, where the index i indicates the angle of measurement. The result (Fig. 3D) shows that the measured mean path length is invariant over nearly two orders of magnitude of transport mean free path. This result is in agreement with the numerical prediction, taking into account the real geometry of the system (glass cell with two interfaces). A small deviation is seen for very weakly scattering samples, where we expect the invariance to hold but where the model underlying our measurement starts to fail. Furthermore, the particles used have diameters of 360 nm, with a pronounced scattering anisotropy (table S1). To test this invariance property also on optically very different systems, the experiment was repeated by using smaller colloidal particles with diameters of 100 nm corresponding to almost isotropic scattering (Fig. 3D, orange curve). Again, the invariance was verified, confirming that neither the transport mean free path nor the anisotropy affect this robust property.

The observed invariance for light scattering in disordered media provides rigid bounds for the optical path length enhancement in multiple scattering media. The relation between the mean optical path length in a medium and the medium's overall geometry provides insights for the optimum design of light-trapping and light-storage devices (*3*, *23*, *24*). Our observation crucially relies on the validity of the equipartition theorem and thus provides a stringent test of this fundamental principle in scattering media. For a medium in which the microstructure strongly modifies the DOS, the mean path length may strongly deviate from our prediction (such as in the bandgap of a photonic crystal) but is recovered by frequency averaging—that is, for sufficiently broadband excitation (*13*). Qualitatively, this can be understood through a connection with known frequency sum rules for the DOS (*25*), showing that over a sufficiently broad spectral range, large and small values of the DOS exactly compensate. Similar deviations are also expected for nanophotonic structures (*26*, *27*) because the Weyl law that was used to derive Eq. 1 only holds in the short-wavelength limit (*13*). The presence of absorption in the medium tends to reduce, and the presence of gain tends to enhance, the weight of longer paths in the path length distribution, in a way that depends, however, on the microstructure of the medium.

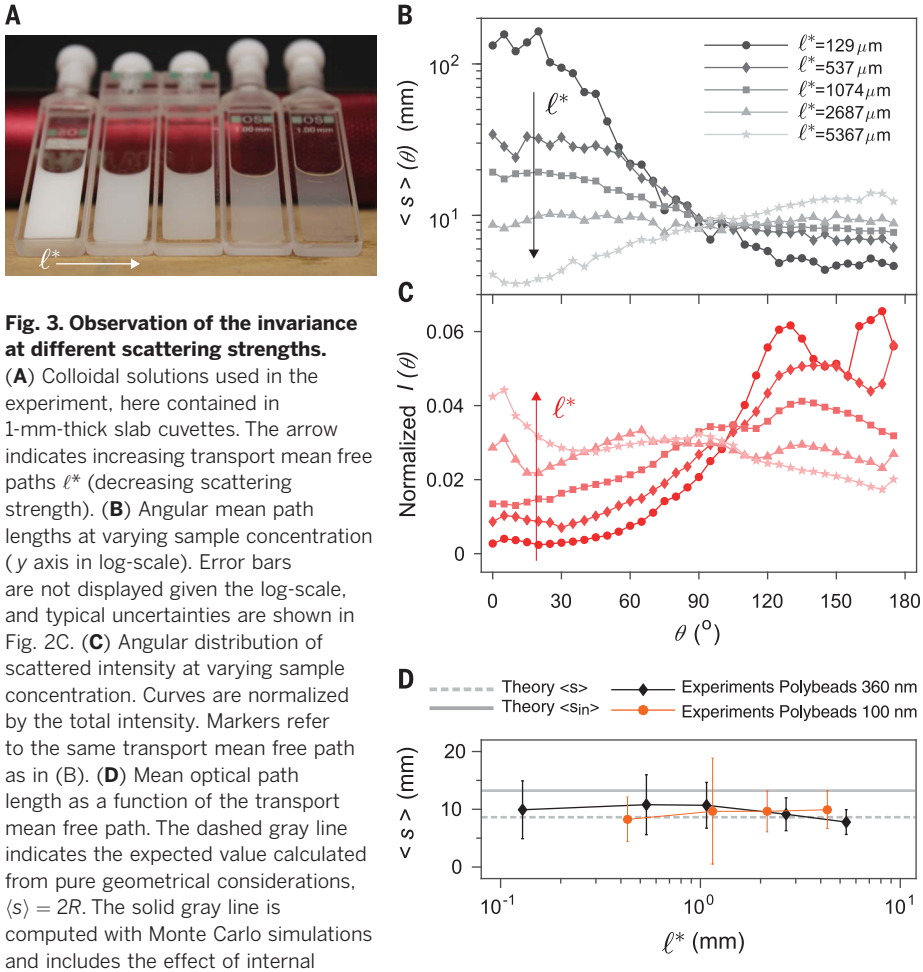

Fig. 3. Observation of the invariance at different scattering strengths. (**A**) Colloidal solutions used in the experiment, here contained in 1-mm-thick slab cuvettes. The arrow indicates increasing transport mean free paths ℓ^* (decreasing scattering strength). (**B**) Angular mean path lengths at varying sample concentration (y axis in log-scale). Error bars are not displayed given the log-scale, and typical uncertainties are shown in Fig. 2C. (**C**) Angular distribution of scattered intensity at varying sample concentration. Curves are normalized by the total intensity. Markers refer to the same transport mean free path as in (B). (**D**) Mean optical path length as a function of the transport mean free path. The dashed gray line indicates the expected value calculated from pure geometrical considerations, $\langle s\rangle = 2R$. The solid gray line is computed with Monte Carlo simulations and includes the effect of internal reflections. Black diamonds represent measurements on polystyrene particles with diameter 360 nm and anisotropy $g \approx 0.8$. Orange circles represent measurements on polystyrene particles with diameter 100 nm and anisotropy $g \approx 0.1$. Error bars give 99% statistical confidence and are calculated by propagating the experimental errors that contribute—the error on the linear fit performed in Fig. 2B and errors on the measurements of ℓ^* and D.

Because the path lengths in a medium are intimately connected with a variety of other crucial concepts such as the dwell time (*28*) and the frequency robustness of states in this medium (*29*, *30*), the invariance property established here is expected to be useful also for wavefront-shaping protocols (*12*). Furthermore, our results are restricted neither to light propagation nor to random walks but apply basically to all wave-scattering problems, ranging from matter waves on the smallest length scales to gravitational waves on the largest conceivable dimensions.

REFERENCES AND NOTES

1. J. D. Joannopoulos *et al*, *Nature* **386**, 143–149 (1997).
2. V. Ntziachristos, *Nat. Methods* **7**, 603–614 (2010).
3. A. Polman, H. A. Atwater, *Nat. Mater.* **11**, 174–177 (2012).
4. A. Marshak, A. Davis, *3D Radiative Transfer in Cloudy Atmospheres* (Springer Science & Business Media, 2005).
5. A. Blanco *et al*., *Nature* **405**, 437–440 (2000).
6. H. Hu, A. Strybulevych, J. H. Page, S. E. Skipetrov, B. A. van Tiggelen, *Nat. Phys.* **4**, 945–948 (2008).

7. P. Barthelemy, J. Bertolotti, D. S. Wiersma, *Nature* **453**, 495–498 (2008).
8. M. Florescu, S. Torquato, P. J. Steinhardt, *Proc. Natl. Acad. Sci. U.S.A.* **106**, 20658–20663 (2009).
9. K. Vynck, M. Burresi, F. Riboli, D. S. Wiersma, *Nat. Mater.* **11**, 1017–1022 (2012).
10. O. L. Muskens, J. G. Rivas, R. E. Algra, E. P. A. M. Bakkers, A. Lagendijk, *Nano Lett.* **8**, 2638–2642 (2008).
11. E. Garnett, P. Yang, *Nano Lett.* **10**, 1082–1087 (2010).
12. S. Rotter, S. Gigan, *Rev. Mod. Phys.* **89**, 015005 (2017).
13. R. Pierrat *et al.*, *Proc. Natl. Acad. Sci. U.S.A.* **111**, 17765–17770 (2014).
14. S. Blanco, R. Fournier, *Europhys. Lett.* **61**, 168–173 (2003).
15. E. Yablonovitch, *J. Opt. Soc. Am.* **72**, 899–907 (1982).
16. L. Pattelli, R. Savo, M. Burresi, D. S. Wiersma, *Light Sci. Appl.* **5**, e16090 (2016).
17. R. H. J. Kop, P. de Vries, R. Sprik, A. Lagendijk, *Phys. Rev. Lett.* **79**, 4369–4372 (1997).
18. G. Popescu, A. Dogariu, *Opt. Lett.* **24**, 442–444 (1999).
19. G. Maret, P. E. Wolf, *Z. Phys. B Condens. Matter* **65**, 409–413 (1987).
20. D. J. Pine, D. A. Weitz, P. M. Chaikin, E. Herbolzheimer, *Phys. Rev. Lett.* **60**, 1134–1137 (1988).
21. D. J. Durian, *Phys. Rev. E* **51**, 3350–3358 (1995).
22. K. K. Bizheva, A. M. Siegel, D. A. Boas, *Phys. Rev. E* **58**, 7664–7667 (1998).
23. S. V. Boriskina *et al.*, *J. Opt.* **18**, 073004 (2016).
24. C. Liu *et al.*, *Nat. Photonics* **7**, 473–478 (2013).
25. R. Carminati, J. J. Sáenz, *Phys. Rev. Lett.* **102**, 093902 (2009).
26. Z. Yu, A. Raman, S. Fan, *Proc. Natl. Acad. Sci. U.S.A.* **107**, 17491–17496 (2010).
27. V. Ganapati, O. D. Miller, E. Yablonovitch, *IEEE J. Photovoltaics* **4**, 175–182 (2014).
28. A. Lagendijk, B. A. van Tiggelen, *Phys. Rep.* **270**, 143–215 (1996).
29. J. Carpenter, B. J. Eggleton, J. Schröder, *Nat. Photonics* **9**, 751–757 (2015).
30. W. Xiong *et al.*, *Phys. Rev. Lett.* **117**, 053901 (2016).

ACKNOWLEDGMENTS

The authors thank P. Ambichl, J. Bertolotti, A. Haber, S. Hallegatte, and J. Schwarz for fruitful discussions and C. Francois-Martin, F. Pincet, and T. Narita for technical assistance with the dynamic light scattering machine. This research was supported by the European Research Council (project reference 278025). R.P. and R.C. were supported by LABEX WIFI (Laboratory of Excellence within the French Program "Investments for the Future") under references ANR-10-LABX-24 and ANR-10-IDEX-0001-02 PSL*. S.R. was supported by the Austrian Science Fund (FWF) through project SFB NextLite F49-P10.

SUPPLEMENTARY MATERIALS

www.sciencemag.org/content/358/6364/765/suppl/DC1
Supplementary Text
Figs. S1 to S9
Tables S1 to S3
References (*31–48*)

7 April 2017; resubmitted 23 June 2017
Accepted 3 October 2017
10.1126/science.aan4054

Observation of mean path length invariance in light-scattering media

Romolo Savo, Romain Pierrat, Ulysse Najar, Rémi Carminati, Stefan Rotter and Sylvain Gigan

Science **358** (6364), 765-768.
DOI: 10.1126/science.aan4054

Scattered light, it is all the same

Materials can vary from transparent to opaque depending on the density of scatters within the medium. As light propagates through a material, intuition might suggest that the more scatters there are, the shorter the path along which the light can propagate. Savo *et al.* confirm a recent theoretical proposal that predicts that this is not the case. They shone light through a series of samples of varying scatterer density and found that the average path length that the light traveled was independent of the sample microstructure. This finding should also be applicable to acoustics and matter waves.

Science, this issue p. 765